Capillary Electrophoresis of Poly(amidoamine) Dendrimers: From Simple Derivatives to Complex Multifunctional Medical Nanodevices

Xiangyang Shi, István J. Majoros, and James R. Baker, Jr.*

Center for Biologic Nanotechnology, Department of Internal Medicine, University of Michigan, Ann Arbor, Michigan 48109

Abstract: Multifunctional poly(amidoamine) (PAMAM) dendrimer-based nanodevices provide novel nanoplatforms for targeting, imaging, and treatment of cancers in vitro and in vivo. Generational, skeletal, and substitutional dispersities are always present in dendrimer-based medical nanodevices. Molecular distribution plays a central role for one to evaluate the quality of PAMAM materials for medical applications. Capillary electrophoresis (CE) has been extensively used as a characterization technique to analyze a range of PAMAM dendrimers, from simple PAMAM derivatives to complex multifunctional PAMAM nanodevices. This review reports the recent advances in the analysis and characterization of a variety of PAMAM dendrimer-based nanoparticles ranging from polycationic and polyanionic PAMAM derivatives to PAMAMs of different generations and defined substitutions, and to complex multifunctional PAMAM nanodevices containing targeting ligands, dyes, and drugs. Understanding the structural complexity of dendrimer nanodevices is crucial for their use as multifunctional imaging, targeting, and cancer therapeutic devices, as well as for their use in biosensing, diagnostics, and control of biological systems.

Keywords: Capillary electrophoresis; poly(amidoamine) dendrimers; dendrimer derivatives; multifunctional dendrimer nanodevices; cancer therapeutics

1. Introduction

Dendrimers are synthetic, highly branched, nearly spherical and symmetrical macromolecules with well-defined sizes and compositions. Tailored dendrimers can be synthesized by appropriately selecting the cores, connecting units, branching sites, and terminal groups. Since the pioneering works of the Tomalia, Newkome, and Vögtle groups in the 1980s,[1-4] a surge of interest has been experienced in the synthesis and applications of dendrimers.[5,6] Altering terminal functionalities of commercially available dendrimers, such as poly(amidoamine) dendrimers (Starburst PAMAMs) and poly(propyleneimine) (Astramol, PPI) dendrimers, affords a wide range of potential applications in catalysis,[7] drug delivery,[8,9]

* To whom correspondence should be addressed. Mailing address: Center for Biologic Nanotechnology, Department of Internal Medicine, University of Michigan, Ann Arbor, MI 48109. E-mail: jbakerjr@umich.edu. Tel: 734 647 2777. Fax: 734 936 2990.

(1) Tomalia, D. A.; Baker, H.; Dewald, J. R.; Hall, M.; Kallos, G.; Martin, S.; Roeck, J.; Ryder, J.; Smith, P. A New Class of Polymers: Starburst-Dendritic Macromolecules. *Polym. J.* **1985**, *17*, 117.

(2) Tomalia, D. A.; Baker, H.; Dewald, J.; Hall, M.; Kallos, G.; Martin, S.; Roeck, J.; Ryder, J.; Smith, P. Dendritic Macromolecules: Synthesis of Starburst Dendrimers. *Macromolecules* **1986**, *19*, 2466-2468.

(3) Newkome, G. R.; Yao, Z. Q.; Baker, G. R.; Gupta, V. K. Cascade Molecules: A New Approach to Micelles. A [27]-Arborol. *J. Org. Chem.* **1985**, *50*, 2003.

(4) Buhleier, E.; Wehner, W.; Vögtle, F. "Cascade" and "Nonskid-Chain-like" Syntheses of Molecular Cavity Topologies. *Synthesis* **1978**, 155-158.

(5) Newkome, G. R.; Moorefield, C. N.; Vögtle, F. *Dendritic Molecules: Concepts, Syntheses, Perspectives*; Wiley-VCH: New York, 1997.

(6) Tomalia, D. A.; Frechet, J. M. J. *Dendrimers and Other Dendritic Polymers*; John Wiley & Sons Ltd: New York, 2001.

sensors,[10−12] optics,[13] electronics,[14,15] and environmental remediation.[16−18]

Recent advances in nanomedicine show that dendrimers are a novel class of nanoscale carriers that can be multifunctionally used for targeting, imaging, and treatment of biological systems.[19] The interior cavities of PAMAMs are often used to encapsulate hydrophobic or hydrophilic drugs.[8,20] In order to better control the release rate, imaging, and targeting properties of drugs, the terminal groups of PAMAMs have been functionalized with various moieties, such as drugs, biospecific ligands, and fluorescent tags.[9,21−23] These dendrimer-based nanodevices hold great promise for various biomedical applications, especially for targeted cancer therapy.

As the efforts to synthesize and manufacture various dendrimers intensify, the quality control and characterization aspects of various dendritic macromolecules still offer great challenges. Dendritic polymers are often considered as being close to perfect structures, but practical samples should be handled as narrow-size-distribution and charge-distribution polymers.[24] Generational, skeletal, and substitutional dispersities always exist in both simple PAMAM derivatives and complex PAMAM medical nanodevices. In addition to the routine chemical analysis methods (UV−vis, FTIR, NMR), numerous methods have been employed for the characterization of PAMAM dendrimers including potentiometric titration,[25−27] scattering methods (SAXS, SANS, dynamic light scattering),[28] size exclusion chromatography (SEC),[27] HPLC,[29−31] electrospray ionization mass spectrometry (ESI-

(7) van Manen, H. J.; van Veggel, F. C. J. M.; Reinhoudt, D. N. Non-covalent synthesis of metallodendrimers. *Dendrimers IV: Metal coordination, self-assembly, catalysis*; Springer-Verlag: Berlin, 2001; pp 163−199.

(8) Esfand, R.; Tomalia, D. A. Poly(amidoamine) (PAMAM) dendrimers: from biomimicry to drug delivery and biomedical applications. *Drug Discovery Today* **2001**, *6*, 427−436.

(9) Patri, A. K.; Majoros, I.; Baker, J. R., Jr. Dendritic polymer macromolecular carriers for drug delivery. *Curr. Opin. Chem. Biol.* **2002**, *6*, 466−471.

(10) Kim, C.; Park, E.; Song, C. K.; Koo, B. W. Ferrocene end-capped dendrimer: synthesis and application to CO gas sensor. *Synth. Met.* **2001**, *123*, 493−496.

(11) Koo, B. W.; Song, C. K.; Kim, C. CO gas sensor based on a conducting dendrimer. *Sens. Actuators, B* **2001**, *77*, 432−436.

(12) Miller, L. L.; Kunugi, Y.; Canavesi, A.; Rigaut, S.; Moorefield, C. N.; Newkome, G. R. "Vapoconductivity". Sorption of Organic Vapors Causes Large Increases in the Conductivity of a Dendrimer. *Chem. Mater.* **1998**, *10*, 1751−1754.

(13) Busson, P.; Örtegren, J.; Ihre, H.; Gedde, U. W.; Hult, A.; Andersson, G.; Eriksson, A.; Lindgren, M. Preparation of mesogen-functionalized dendrimers for second-order nonlinear optics. *Macromolecules* **2002**, *35*, 1663−1671.

(14) Ma, D.; Lupton, J. M.; Beavington, R.; Burn, P. L.; Samuel, I. D. W. Improvement of luminescence efficiency by electrical annealing in single-layer organic light-emitting diodes based on a conjugated dendrimer. *J. Phys. D: Appl. Phys.* **2002**, *35*, 520−523.

(15) Ma, H.; Chen, B.; Sassa, T.; Dalton, L. R.; Jen, A. K. Highly efficient and thermally stable nonlinear optical dendrimer for electrooptics. *J. Am. Chem. Soc.* **2001**, *123*, 986−987.

(16) Diallo, M. S.; Christie, S.; Swaminathan, P.; Johnson, J. H., Jr.; Goddard, W. A., III. Dendrimer Enhanced Ultrafiltration. 1. Recovery of Cu(II) from Aqueous Solutions Using PAMAM Dendrimers with Ethylene Diamine Core and Terminal NH2 Groups. *Environ. Sci. Technol.* **2005**, *39*, 1366−1377.

(17) Diallo, M. S.; Christie, S.; Swaminathan, P.; Balogh, L.; Shi, X.; Um, W.; Papelis, C.; Goddard, W. A., III; Johnson, J. H., Jr. Dendritic Chelating Agents. 1. Cu(II) Binding to Ethylene Diamine Core Poly(amidoamine) Dendrimers in Aqueous Solutions. *Langmuir* **2004**, *20*, 2640−2651.

(18) Diallo, M. S.; Balogh, L.; Shafagati, A.; Johnson, J. H., Jr.; Goddard, W. A., III; Tomalia, D. A. Poly(amidoamine) Dendrimers: A New Class of High Capacity Chelating Agents for Cu(II) Ions. *Environ. Sci. Technol.* **1999**, *33*, 820−824.

(19) Moghimi, S. M.; Hunter, A. C.; Murry, J. C. Nanomedicine: current status and future prospects. *FASEB J.* **2005**, *19*, 311−330.

(20) Beezer, A. E.; King, A. S. H.; Martin, I. K.; Mitchel, J. C.; Twyman, L. J.; Wain, C. F. Dendrimers as potential drug carriers; encapsulation of acidic hydrophobes within water soluble PAMAM derivatives. *Tetrahedron* **2003**, *59*, 3873−3880.

(21) Quintana, A.; Raczka, E.; Piehler, L.; Lee, I.; Myc, A.; Majoros, I.; Patri, A. K.; Thomas, T.; Mule, J.; Baker, J. R., Jr. Design and function of a dendrimer-based therapeutic nanodevice targeted to tumor cells through the folate receptor. *Pharm. Res.* **2002**, *19*, 1310−1316.

(22) Baker, J. R., Jr.; Quintana, A.; Piehler, L. T.; Banazak-Holl, M.; Tomalia, D.; Raczka, E. The synthesis and testing of anti-cancer therapeutic nanodevices. *Biomed. Microdevices* **2001**, *3*, 61−69.

(23) Majoros, I. J.; Thomas, T. P.; Baker, J. R., Jr. Molecular Engineering in Nanotechnology: Engineered Drug Delivery. In *Handbook of Theoretical and Computational Nanotechnology*; Rieth, M., Schommers, W., Eds.; American Scientific Publishers: Stevenson Ranch, CA, in press.

(24) Zhou, L.; Russell, D. H.; Zhao, M.; Crooks, R. M. Characterization of Poly(amidoamine) Dendrimers and Their Complexes with Cu²⁺ by Matrix-Assisted Laser Desorption Ionization Mass Spectrometry. *Macromolecules* **2001**, *34*, 3567−3573.

(25) Shi, X.; Bányai, I.; Lesniak, W.; Islam, M. T.; Országh, I.; Balogh, P.; Baker, J. R., Jr.; Balogh, L. Capillary Electrophoresis of Polycationic Poly(amidoamine) Dendrimers. *Electrophoresis*, in press.

(26) Shi, X.; Patri, A. K.; Lesniak, W.; Islam, M. T.; Zhang, C.; Baker, J. R., Jr.; Balogh, L. Analysis of Polyamidoamine-Succinamic Acid Dendrimers by Slab-Gel Electrophoresis and Capillary Zone Electrophoresis. *Electrophoresis*, in press.

(27) Majoros, I. J.; Keszler, B.; Woehler, S.; Bull, T.; Baker, J. R., Jr. Acetylation of Poly(amidoamine) Dendrimers. *Macromolecules* **2003**, *36*, 5526−5529.

(28) Tan, N. C. B.; Balogh, L.; Trevino, S. F.; Tomalia, D. A.; Lin, J. S. A small angle scattering study of dendrimer-copper sulfide nanocomposites. *Polymer* **1999**, *40*, 2537−2545.

(29) Choi, Y.; Thomas, T.; Kotlyar, A.; Islam, M. T.; Baker, J. R., Jr. Synthesis and functional evaluation of DNA-assembled polyamidoamine dendrimer clusters for cancer cell-specific targeting. *Chem. Biol.* **2005**, *12*, 35−43.

(30) Islam, M. T.; Shi, X.; Balogh, L.; Baker, J. R., Jr. HPLC Separation of Different Generations of Poly(amidoamine) Dendrimers Modified with Various Terminal Groups. *Anal. Chem.* **2005**, *77* (7), 2063−2070.

(31) Islam, M. T.; Majoros, I. J.; Baker, J. R., Jr. HPLC Analysis of PAMAM Dendrimer Based Multifunctional Devices. *J. Chromatogr., B: Anal. Technol. Biomed. Life Sci.*, in press.

MS), and matrix-assisted laser desorption ionization time-of-flight (MALDI-TOF) mass spectrometric (MS) methods.[32−34]

Capillary electrophoresis (CE) is a powerful chromatographic method utilized in the analysis of biologic macromolecules, such as DNA,[35] proteins,[36] peptides,[37] etc. CE has high efficiency, high sensitivity, short run time, and high automation capability, and it is suitable for the routine analysis of diverse dendrimer architectures, especially those that are carrying multiple charges. This review reports the recent advances of CE analysis and characterization of various PAMAM dendrimer nanomaterials from simple PAMAM derivatives to complex multifunctional PAMAM nanodevices. The CE analysis of dendrimers other than PAMAMs is beyond the scope of this review and is not included herein. Unless otherwise stated, all the PAMAM dendrimers reported here have ethylenediamine (EDA) cores.

2. Capillary Electrophoresis

CE is a fast and reliable practical analytical technique.[38] The separation of macromolecules is mainly based on the difference of their charge/mass ratios under practical conditions although some other factors may influence their separation such as hydrodynamic radius, counterion binding, and the adsorption/desorption of macromolecules onto the capillary surface. CE can provide data of theoretical interest as well as molecular distribution for PAMAM dendrimers, the main question being how much charge the dendrimer molecules in fact carry in solution. For example, amine-terminated PAMAM dendrimers may carry a large number of positive charges when protonated and their high generations display particle-like characteristics. Fully modified PAMAM dendrimers contain interior tertiary amines, which are protonated under lower pH conditions, and carry multiple positive charges. Multifunctional PAMAM nanodevices bearing multiple surface ligands display significantly low charge/mass ratios because of the multiple surface conjugations with functional moieties. Compared with other techniques (e.g., NMR, UV−vis spectrometry, HPLC) which generally reflect average molecular events, the variation and slight modification of PAMAM terminal groups can be magnified and sensitively detected using CE, mainly based on the change of charge/mass ratios.

3. Capillary Electrophoresis of Amine-Terminated PAMAM Dendrimers

Amine-terminated PAMAM dendrimers are always used as the starting materials for preparation of PAMAM derivatives and multifunctional PAMAM nanodevices. Understanding the structural deviation is crucial for one to characterize complex PAMAM nanodevices for biomedical application. Commercially available amine-terminated PAMAMs always contain trailing generations and intermolecularly coupled dendrimers (referred to as generational dispersity), as well as missing arms and molecular loops (referred to as skeletal dispersity), which result from side reactions during the divergent synthetic processes. Only a limited number of reports have been published regarding the analysis of dendrimers by using CE.[39−47]

Using a simple model for CE allows us to directly estimate the effective charge that various PAMAM dendrimers experience under CE conditions. When a particle moves with constant velocity, the sum of all forces on that particle must

(32) Schwartz, B. L.; Rockwood, A. L.; Smith, R. D.; Tomalia, D. A.; Spindler, R. Detection of high molecular weight starburst dendrimers by electrospray ionization mass spectrometry. *Rapid Commun. Mass Spectrom.* **1995**, *9*, 1552−1555.
(33) Kallos, G. J.; Lewis, S.; Zhou, J.; Hedstrand, D. M.; Tomalia, D. A. Molecular Weight Determination of a Polyamidoamine Starburst Polymer by Electrospray Ionization Mass Spectrometry. *Rapid Commun. Mass. Spectrom.* **1991**, *5*, 383.
(34) Woller, E. K.; Cloninger, M. J. Mannose Functionalization of a Sixth Generation Dendrimer. *Biomacromolecules* **2001**, *2*, 1052−1054.
(35) Mitnik, L.; Novotny, M.; Felten, C. Recent advances in DNA sequencing by capillary and microdevice electrophoresis. *Electrophoresis* **2001**, *22*, 4104−4117.
(36) Patrick, J. S.; Lagu, A. L. Review applications of capillary electrophoresis to the analysis of biotechnology-derived therapeutic proteins. *Electrophoresis* **2001**, *22*, 4179−4196.
(37) Righetti, P. G. Capillary electrophoretic analysis of proteins and peptides of biomedical and pharmacological interest. *Biopharm. Drug Dispos.* **2001**, *22*, 337−351.
(38) Li, S. F. Y. *Capillary Electrophoresis Theory & Practice*; Academic Press: San Diego, 1992.
(39) Brothers, H. M.; Piehler, L. T.; Tomalia, D. A. Slab-gel and capillary electrophoretic characterization of polyamidoamine dendrimers. *J. Chromatogr., A* **1998**, *814*, 233−246.
(40) Ebber, A.; Vaher, M.; Peterson, J.; Lopp, M. Application of capillary zone electrophoresis to the separation and characterization of poly(amidoamine) dendrimers with an ethylenediamine core. *J. Chromatogr., A* **2002**, *949*, 351−358.
(41) Balogh, L.; de Leuze-Jallouli, A.; Dvornic, P.; Kunugi, Y.; Blumstein, A.; Tomalia, D. A. Architectural copolymers of PAMAM dendrimers and ionic polyacetylenes. *Macromolecules* **1999**, *32*, 1036−1042.
(42) Tomalia, D. A.; Huang, B.; Swanson, D. R.; Brothers, H. M.; Klimash, J. W. Structure control within poly(amidoamine) dendrimers: size, shape and regio-chemical mimicry of globular proteins. *Tetrahedron* **2003**, *59*, 3799−3813.
(43) Pesak, D. J.; Moore, J. S.; Wheat, T. E. Synthesis and characterization of water-soluble dendritic macromolecules with a stiff, hydrocarbon interior. *Macromolecules* **1997**, *30*, 6467−6482.
(44) Castagnola, M.; Zuppi, C.; Rossetti, D. V.; Vincenzoni, F.; Lupi, A.; Vitali, A.; Meucci, E.; Messana, I. Characterization of dendrimer properties by capillary electrophoresis and their use as pseudostationary phases. *Electrophoresis* **2002**, *23*, 1769−1778.
(45) Huang, Q. R.; Dubin, P. L.; Moorefield, C. N.; Newkome, G. R. Counterion binding on charged spheres: Effect of pH and ionic strength on the mobility of carboxyl-terminated dendrimers. *J. Phys. Chem. B* **2000**, *104*, 898−904.
(46) Seyrek, E.; Dubin, P. L.; Newkome, G. R. Effect of electric field on the mobility of carboxyl-terminated dendrimers. *J. Phys. Chem. B* **2004**, *108*, 10168−10171.
(47) Welch, C. F.; Hoagland, D. A. The electrophoretic mobility of PPI dendrimers: Do charged dendrimers behave as linear polyelectrolytes or charged spheres? *Langmuir* **2003**, *19*, 1082−1088.
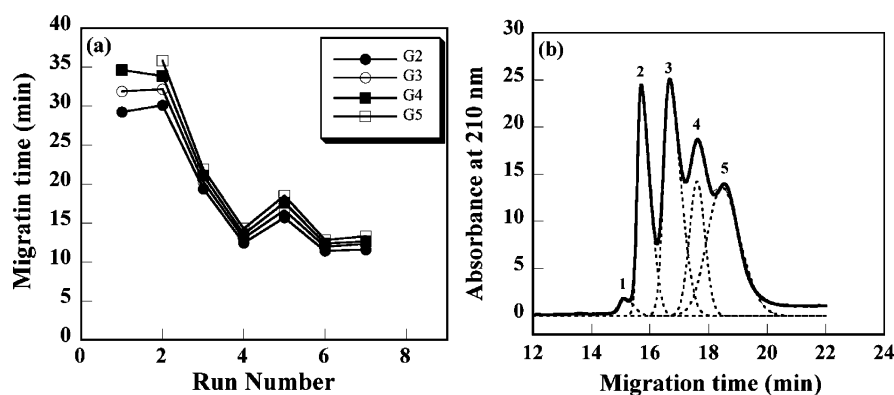
Figure 1. (a) Relationship between the migration times of $G2.NH_2$, $G3.NH_2$, $G4.NH_2$, and $G5.NH_2$ separated using a bare fused silica capillary as a function of consecutive run numbers. (b) A typical capillary electropherogram of the mixture of EDA core amine-terminated PAMAM dendrimers of generations 2−5 using the same capillary (i.d. 100 μm, total length 78.5 cm, and effective length 70 cm). Injection time: 3 s. Original data is the real electropherogram, and generated data was obtained from the PeakFit program. They are overlapped. Peaks 1, 2, 3, 4, and 5 correspond to the $G1.NH_2$ trace (in the $G2.NH_2$ dendrimer), $G2.NH_2$, $G3.NH_2$, $G4.NH_2$, and $G5.NH_2$.

be zero. At pH = 2.5 when a protonated and positively charged $GX.NH_2$ (G refers to generation, and X refers to the generation number) PAMAM dendrimer molecule moves in a capillary by means of an electric field toward the cathode, the following main effects should be considered. First, the electric force (F_e) consists of two components: an electrophoretic and an electroosmotic part. The latter is negligible under our conditions because, at this pH, the wall of the silica capillary is neutral. Second, there is a hydrodynamic force, which comes from the different types of "friction" of the medium (hydrodynamic friction or viscosity and the dynamics of counterion cloud, or relaxation effect). The mobility of the dendrimers can be written in eq 1 in a dimensionless form:

$$\mu_0' = \frac{\mu_0 3\eta e}{2\epsilon\epsilon_0 kT} = \frac{lL}{Vt_m}\frac{3\eta e}{2\epsilon\epsilon_0 kT} \tag{1}$$

where l is the effective length (cm), L is the total length (cm), V is the voltage (V), t_m is the migration time (s), μ_0 is the electrophoretic mobility (cm^2 V^{-1} s^{-1}), ϵ is the dielectric constant of water (80.5), ϵ_0 is the dielectric permittivity of the vacuum, k is the Boltzmann constant, T is the temperature, η is the viscosity, and e is charge of the electron.

Dendrimers are believed to be the first experimental example of moving charged spheres for which the Hückel−Smoluchowski theory[48] works rather well. Huang et al.[45] found that, in the case of carboxylic acid terminated cascade dendrimers, the large negative charge of the macromolecule is partially compensated by counterion binding to the spherical molecules, which is analogous to the Manning hypothesis[49] about counterion condensation on polyelectrolytes. Recently, Welch and Hoagland[47] have reported that

poly(propylenimine) (PPI) dendrimers can be considered as moving charged spheres. Three factors are dominant in the motion of these spherical macromolecules toward the cathode: the electric field, the hydrodynamic friction, and the relaxation effect of the counterion cloud. PAMAM dendrimers carrying the same number of nitrogen atoms are much larger than the corresponding PPI dendrimers. Therefore, if there is a counterion effect, it should be more pronounced for PAMAMs than for PPI dendrimers.

Brothers et al.[39] and Ebber et al.[40] recently reported the application of capillary zone electrophoresis to separate and characterize PAMAM dendrimers using bare fused silica capillary. The measured migration times of polycationic PAMAM dendrimers were not reproducible. It is known that polycationic PAMAM dendrimers have a strong tendency to be adsorbed onto negatively charged silica or glass surfaces.[50−52] It has been reported that the pK_a values of the terminal primary amine groups and the tertiary amine groups of PAMAM dendrimers are between 9 and 10 and between 4 and 5, respectively.[1,53] At low-pH conditions (pH < 3.0), when all amine groups in a PAMAM molecule are proto-

(48) Loeb, A. L.; Overbeek, J. T. G.; Wiersema, P. H. *The Electrical Double Layer Around a Spherical Colloid Particle*; MIT Press: Cambridge, 1961.

(49) Manning, G. S. Limiting Laws and Counterion Condensation in Polyelectrolyte Solutions. I. Colligative Properties. *J. Chem. Phys.* **1969**, *51*, 924.

(50) Esumi, K.; Goino, M. Adsorption of Poly(amidoamine) Dendrimers on Alumina/Water and Silica/Water Interfaces. *Langmuir* **1998**, *14*, 4466−4470.

(51) Ottaviani, M. F.; Turro, N. J.; Jockusch, S.; Tomalia, D. A. EPR Investigation of the Adsorption of Dendrimers on Porous Surfaces. *J. Phys. Chem. B* **2003**, *107*, 2046−2053.

(52) Tsukruk, V. V.; Rinderspacher, F.; Bliznyuk, V. N. Self-Assembled Multilayer Films from Dendrimers. *Langmuir* **1997**, *13*, 2171−2176.

(53) Tomalia, D. A.; Naylor, A. M.; Goddard, W. A., III. Starburst dendrimers: control of size, shape, surface chemistry, topology and flexibility in the conversion of atoms to macroscopic materials. *Angew. Chem., Int. Ed. Engl.* **1990**, *29*, 138.
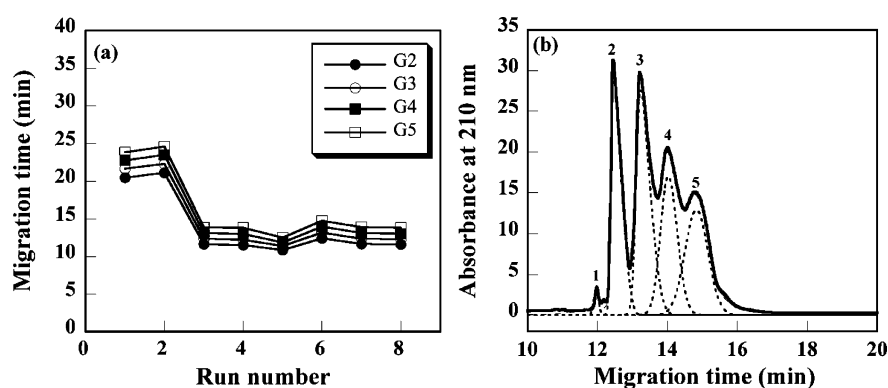
Figure 2. (a) Relationship between the migration times and the consecutive run numbers for the G2.NH$_2$, G3.NH$_2$, G4.NH$_2$, and G5.NH$_2$ dendrimers separated on a silanized silica capillary. (b) A typical capillary electropherogram of the mixture of EDA core amine-terminated PAMAM dendrimers of generations 2−5 using the same silanized silica capillary (i.d. 100 μm, total length 78.5 cm, and effective length 70 cm). Injection time: 3 s. Original data is the real electropherogram, and generated data was obtained from the PeakFit program. They are overlapped. Peaks 1, 2, 3, 4, and 5 correspond to the G1.NH$_2$ trace (in the G2.NH$_2$ dendrimer), G2.NH$_2$, G3.NH$_2$, G4.NH$_2$, and G5.NH$_2$.

nated,[54] adsorption of dendrimers onto the capillary wall surface[55] makes the separation irreproducible.

In order to decrease the adsorption of PAMAM dendrimers onto the capillary surface, a silanization reaction has been performed by reacting the silanol groups of the capillary surface with chlorotrimethylsilane, which renders the capillary surface with hydrophobic methyl groups.[25] This has been proved to significantly reduce the adsorption of PAMAM dendrimers onto a silica substrate.[56] The reproducibility of the separation of primary amine terminated ("full-generation") PAMAMs, using both native silica and silanized capillary, has been compared (Figure 1 and Figure 2).[25] Migration times of dendrimers are clearly decreasing in the consecutive runs approaching a plateau. The long migration times (30−35 min) (see Figure 1a) of the first two runs indicate strong binding of PAMAM dendrimers to the silica wall. After an initial "conditioning" of the capillary, a dynamic equilibrium develops and the PAMAM migration times become very similar to the ones in the previous runs. Figure 1b shows the achievable separation of the primary amine terminated PAMAM generations G2.NH$_2$, G3.NH$_2$, G4.NH$_2$, and G5.NH$_2$ using a bare fused silica capillary in the fifth run. Silanization of the capillary surface may decrease the number of active centers and not only leads to faster equilibration but also clearly makes the separation more reproducible. When silanized capillary was used for the separation of the same mixture of PAMAM dendrimers (Figure 2a), the migration times rapidly decreased in

subsequent injections and stabilized at steady values. A typical separation at run 6 is shown in Figure 2b, for G2.NH$_2$, G3.NH$_2$, G4.NH$_2$, and G5.NH$_2$ separated from their mixture.

To reduce the experimental error, an internal standard has been employed to normalize the migration times of PAMAMs of different generations. 2,3-Diaminopyridine (2,3-DAP) proved to be a good internal standard. Figure 3 compares uncorrected (Figure 3a) and normalized (Figure 3b) electropherograms of G2.NH$_2$, G4.NH$_2$, and G5.NH$_2$ PAMAMs in the presence of 2,3-DAP. The normalized curves clearly reflect the change in the mobility of the investigated dendrimers, and the relative mobility of G5.NH$_2$ is smaller than that of G4.NH$_2$. The apparent electrophoretic mobility can be calculated according to the following equation:

$$\mu_0 = \frac{lL}{Vt_{\mathrm{m}}} \tag{2}$$

where l is the effective length of the capillary (from inlet to detector window), L is the total length of the capillary (both in cm), V is the applied voltage (V), and t_{m} is the migration time (s). According to the known migration time of 2,3-DAP ($t_{\mathrm{M}} = 11.80$ min, the average of 6 different runs), the electrophoretic mobilities of G4.NH$_2$ and G5.NH$_2$ were calculated as 3.63×10^{-5} cm^2 V^{-1} s^{-1} and 3.50×10^{-5} cm^2 V^{-1} s^{-1}, respectively.

Although the charge/mass ratio values are almost constant on the basis of both theoretical calculation and practical measurements (from acid−base titration and GPC data, their actual charge/mass ratios range from 0.0066 to 0.0087), amine-terminated PAMAMs of different generations separate, due to the adsorption/desorption of dendrimers on the capillary surface. There are also secondary factors to contribute generational separation: e.g., smaller generation PAMAM dendrimers may have a smaller contact area but higher flexibility to promote adsorption onto the capillary

(54) Cakara, D.; Kleimann, J.; Borkovec, M. Microscopic Protonation Equilibria of Poly(amidoamine) Dendrimers from Macroscopic Titrations. *Macromolecules* **2003**, *36*, 4201−4207.

(55) Weinberger, R. The evolution of capillary electrophoresis: Past, present, and future. *Am. Lab.* **2002**, *34*, 32−40.

(56) Betley, T. A.; Holl, M. M. B.; Orr, B. G.; Swanson, D. R.; Tomalia, D. A.; Baker, J. R., Jr. Tapping Mode Atomic Force Microscopy Investigation of Poly(amidoamine) Dendrimers: Effects of Substrate and pH on Dendrimer Deformation. *Langmuir* **2001**, *17*, 2768−2773.
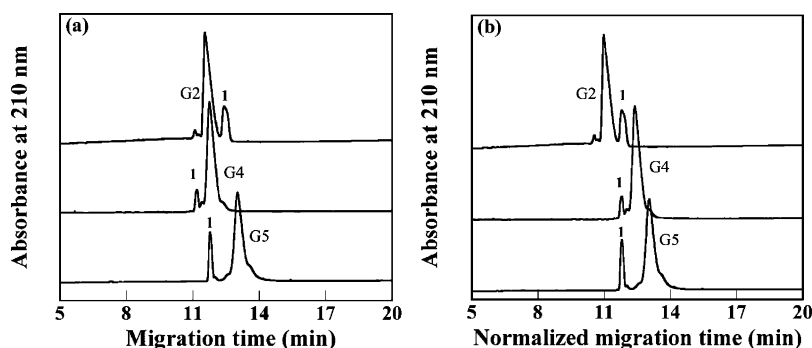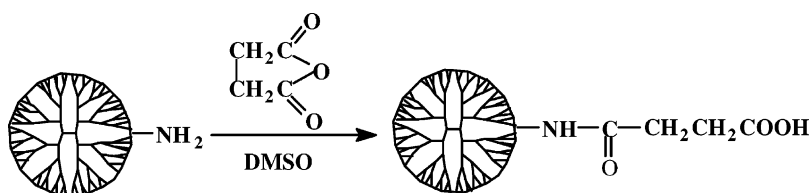
Figure 3. Comparison of uncorrected (a) and normalized (b) electropherograms of the G2.NH$_2$, G4.NH$_2$, and G5.NH$_2$ PAMAM dendrimers in the presence of the 2,3-DAP internal standard using a silanized capillary (i.d. 100 μm, effective length 70 cm, and total length 78.5 cm). Peak 1 indicates the internal standard 2,3-DAP. Injection time: 3 s.

Scheme 1. Schematic Representation of the Synthesis of PAMAM-SAs

surface, while higher generations have a larger contact area, but are more rigid.[57]

As a summary, a chromatographic method was developed for the analysis and characterization of amine-terminated PAMAM dendrimers of different generations using CE. Separation and characterization is more reproducible on a silanized capillary than on uncoated capillary. 2,3-DAP was chosen as an internal standard for polycationic PAMAM analysis. Ratios of migration times to standards proved to be very reproducible. Our measurements show that although the electric field moves the polycationic dendrimers in the capillary, the retention differences are dominantly due to the interactions of the PAMAM dendrimers with the capillary wall. It is concluded that for polycationic PAMAMs a complex separation mechanism has to be considered, which is in character close to the electrokinetic capillary chromatography.

4. Capillary Electrophoresis of Carboxyl-Terminated PAMAM Dendrimers

PAMAM-succinamic acids (PAMAM-SAs) are a new group of polyanionic PAMAM derivatives that can be used for the synthesis of dendrimer-based therapeutic nanodevices,[21] and they have been used in the synthesis of complex core−shell tecto(dendrimers).[58] However, there is no data reported on CE analysis of this group of polyanionic

PAMAMs. Compared with "half-generation" carboxylterminated PAMAM dendrimers made by hydrolysis of methyl esters,[39] PAMAM-SAs have the following advantages: (1) the modification step is simple and more controllable, (2) the polydispersity of PAMAM-SAs is much lower than that of the half-generation PAMAM carboxylates,[39] and (3) the number of terminal carboxyl groups remains identical to that of primary amine groups of the starting full-generation dendrimers, which makes comparisons between parent dendrimers and derivatives easier.

As opposed to the analysis of amine-terminated PAMAMs, there is no electrostatic interaction between negatively charged PAMAM-SAs and the negatively charged silica capillary surface. In this case, a bare silica capillary was used for the analysis of PAMAM-SA dendrimers. We synthesized PAMAM-SA dendrimers of generations 1 through 7 (Scheme 1) and a core−shell tecto(dendrimer) G5(G3.SA)$_n$[58] and characterized them by polyacrylamide gel electrophoresis (PAGE) and CE.[26] Native PAGE and sodium dodecyl sulfate (SDS)−PAGE permitted the evaluation of dendrimer quality and molecular mass, while CE provided information about the dependence of electrophoretic mobility as a function of dendrimer generations. The combination of PAGE and CE analysis presents an effective strategy to characterize polyanionic PAMAM-SA dendrimers.

Figure 4 shows the PAGE electropherogram of generations 3 through 7 of PAMAM-SAs obtained on a gradient (4−20%) polyacrylamide gel. At the pH of the PAGE buffer (pH = 8.3), tertiary amines (pK_a = 4−5) are not protonated,[2,53] while the terminal carboxyl groups are deprotonated, endowing them with multiple negative charges. Therefore, PAMAM-SA molecules migrate toward the anode in an electric field. It is clear that the smaller sized lower generation molecules migrate faster than their higher genera-

(57) Rahman, K. M. A.; Durning, C. J.; Turro, N. J.; Tomalia, D. Adsorption of poly(amidoamine) dendrimers on gold. *Langmuir* **2000**, *16*, 10154−10160.

(58) Uppuluri, S.; Swanson, D. R.; Piehler, L. T.; Li, J.; Hagnauer, G. L.; Tomalia, D. A. Core-Shell Tecto(dendrimers): I. Synthesis and Characterization of Saturated Shell Models. *Adv. Mater.* **2000**, *12*, 796−800.
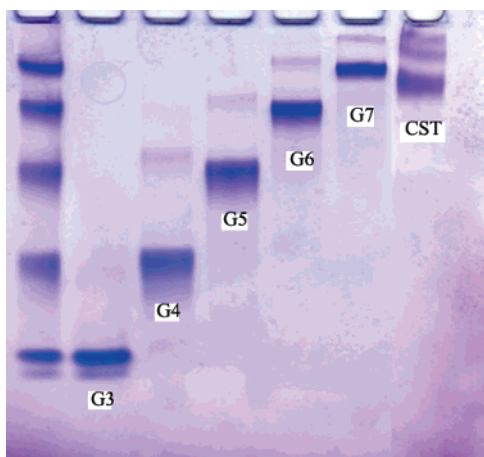
Figure 4. PAGE electropherograms of EDA-core PAMAM-SA dendrimers of different generations (3–7) and a core(G5)–shell(G3) tecto(dendrimer) (CST) analyzed on a 4–20% gradient polyacrylamide gel using tris-glycine native buffer. The unlabeled lane shows the separation of a mixture composed of G3.SA–G7.SA. The generations ascend from 3 through 7 from left to right.

tion congeners. From Figure 4, it is also clear that each generation of PAMAM-SAs is flanked by its next higher generations on the electropherograms. Full-generation PAMAMs always contain a small amount of dimers that appear in the PAGE electropherogram in the same position as the next generation dendrimer (the MW almost exactly doubles between generations.).[39] Thus, as PAMAM-SAs are derived from full-generation amine-terminated PAMAMs, dimers and higher intermolecular coupling impurities are also present in the products. Although the molecular mass of dimers of each generation of PAMAM-SA dendrimers is almost identical to that of the next higher generation PAMAM-SAs, this is not necessarily reflected in the PAGE electropherogram due to the difference between their molecular shapes. Dimers of PAMAM-SAs are expected to exhibit larger lateral size than their next higher PAMAM-SAs do, which may slightly block their migration under the same electrophoresis conditions. The migration distance of the G5(G3.SA)$_n$ CST shown in the rightmost lane is between G6.SA and G7.SA, indicating that its molecular mass is between that of G6.SA and that of G7.SA. In addition, the mixture of generations in the leftmost lane is also well separated, suggesting that preparative electrophoretic separation can potentially provide relatively pure materials for downstream studies and applications.

Quantitative analysis of PAMAM dendrimers can be performed using CE. To compare PAGE results with those obtained by CE, the pH was maintained at 8.3 with 20 mM borate buffer. Figure 5 shows the electropherograms of PAMAM-SAs of generations 3–7. In contrast to the multiple peaks present in the CE electropherograms of half-generation carboxyl-terminated PAMAM dendrimers derived from hydrolysis of PAMAM half-generation esters,[44] all PAMAM-SAs (generations 3–7) displayed a single, symmetric peak. Dimers or higher intermolecular impurities that appeared in

PAGE electropherograms (Figure 4) are absent from the CE electropherograms, which is due to the fact that their charge/mass ratios are similar to those of single dendrimer molecules and the CZE mode cannot differentiate between molecular sizes. However, for lower generation PAMAM-SAs of generation 1, there are multiple peaks present in the electropherogram before the main peak. This may be attributable to the presence of a trailing generation (generation 0) and other imperfect dendrimer species converted into SA derivatives from the starting primary amine terminated generation 1 dendrimer. The charge/mass ratio of these dendrimer species can be differentiated at the generation 1 level when the respective charge/mass ratios are different from each other. With the increase in the number of dendrimer generations, the charge/mass ratio differences of the trailing generations and imperfect structures become smaller and smaller. Accordingly, for G2.SA, there is only one peak appearing before the main peak, and for G3.SA through G7.SA, only a single symmetric dendrimer peak is present in the electropherograms, even though PAGE detects the presence of minute amounts of different species (trailing generations and dimers) in the samples. Another possible reason is related to the manufacture of the starting primary amine terminated dendrimers, during which lower generations (generations 0–2) are not purified by the ultrafiltration process; therefore the purity of their succinamic acid derivatives is relatively low. The impure nature of lower generations of amine-terminated PAMAMs has been confirmed in the literature using CE.[40]

We also measured how the electrophoretic mobility of PAMAM-SAs changes as a function of generation number. Figure 5b (normalized electropherograms of G3.SA, G4.SA, G5.SA, G6.SA, G7.SA) indicates that all these polyanionic dendrimers have very similar electrophoretic mobilities. Electrophoretic mobilities are in the range of $(3.6–4.1) \times 10^{-4}$ cm^2 V^{-1} s^{-1}. The similarity of electrophoretic mobilities is believed to result from their nearly identical charge/mass ratios.[26] Consequently, a mixture of G3.SA, G4.SA, G5.SA, G6.SA, and G7.SA cannot be separated under these conditions and only a single peak appears in the electropherogram. These results are very different from those observed for polycationic PAMAM dendrimers. For amine-terminated PAMAMs, we found that increasing generation numbers results in decreasing mobility, and we concluded that adsorption of the polycationic dendrimers on the capillary wall surface is responsible for the separation.[25] Polyanionic carboxyl-terminated dendrimers are not adsorbed onto the surface of the negatively charged silica capillary during separation, and only the charge/mass ratio and electroosmotic flow (EOF) affect the separation.

Core–shell tecto(dendrimers) are one of the possible structures for multifunctional dendrimer nanodevices. Figure 6 shows the electropherogram of a G5(G3.SA)$_n$ tecto-(dendrimer) carrying carboxyl terminal groups ($M_{n(SEC)} = 152\,200$, $M_w/M_n = 1.196$). The theoretical charge/mass ratio of this tectodendrimer is 1.74×10^{-3} mol/g, which is very close to the practical value (1.94×10^{-3} mol/g) based on
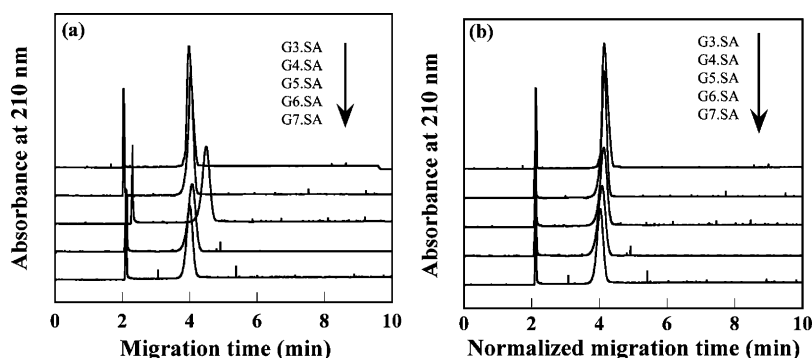
Figure 5. Electropherograms (a) and normalized electropherograms (b) of PAMAM-SAs of generations 3−7 analyzed using a bare fused silica capillary (i.d. 75 μm, effective length 40 cm, and total length 48.5 cm). Injection time: 3 s. The first peak in all electropherograms corresponds to mesityl oxide (MO), which was used as a neutral marker. The normalized CE electropherogram was based on the average migration time of the neutral marker (2.12 min, run time $n = 23$).
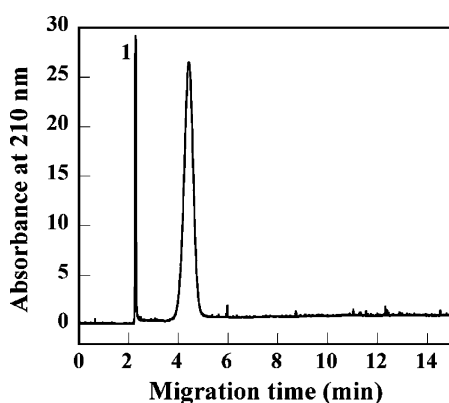

Figure 6. Electropherogram of G5(G3.SA)$_{12}$, a core−shell-SA tecto(dendrimer). Peak 1 indicates mesityl oxide, the neutral marker.

Figure 7. Normalized CE electropherograms of G1.NH$_2$, G1.NHAc, and G1.N(Gly)OH (normalized migration time of the internal standard, $t_{IS} = 9.20$ min, the average value of 7 runs, detection wavelength at 210 nm). Peak 1: 2,3-diaminopyridine. CE was performed using a bare fused silica capillary (i.d. 75 μm, total length 64.5 cm, and effective length 56 cm). Injection time: $t = 3$ s. Reprinted with permission from ref 61. Copyright 2005 Elsevier Science.

potentiometric titration and SEC measurements. This charge/mass ratio value is considerably lower than that of single-generation PAMAM-SA dendrimers (generations 2−7). Accordingly, G5(G3.SA)$_n$ has an electrophoretic mobility of $(3.42 \pm 0.03) \times 10^{-4}$ cm^2 V^{-1} s^{-1}, which is less than that of the single generations. This observation further supports that only the charge/mass ratio and EOF play a major role in the separation of polyanionic PAMAMs.

In summary, polyanionic PAMAM dendrimers of different generations carrying succinamic acid termini were analyzed by CE and PAGE. PAGE can separate various generations due to the gel filtration effect; thus the purity and homogeneity of the dendrimer material can be assessed. A CZE method was established for PAMAM-SAs which was also applied to a core−shell tecto(dendrimer). The similar electrophoretic mobilities for all generations (1−7) indicate that the polyanionic PAMAMs are not adsorbed on the surface of the quartz capillary; thus only the charge/mass ratio and the EOF influence the separation. The movement of ions mainly depends on the electric field, and minor differences in charge/mass ratios are insufficient to achieve effective separations between generations.
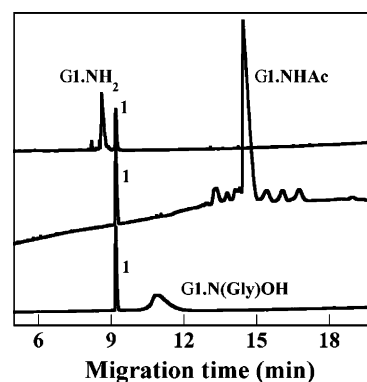
5. Capillary Electrophoresis of PAMAMs of Other Fully Modified Functionalities

Commercial PAMAM dendrimers always contain "trailing generation(s)" as well as dimers, and real PAMAM molecules almost always display missing arms and molecular loops.[25,39,59,60] These defects result from the four main types of side reactions during the synthesis: (1) a retro-Michael reaction gives rise to asymmetrical structures due to missing arms; (2) dimers may form in the amidation step by intermolecular coupling and (3) intramolecular cyclization (intramolecular coupling) may also occur during the same

(59) Sharma, A.; Mohanty, D. K.; Desai, A.; Ali, R. A simple polyacrylamide gel electrophoresis procedure for separation of polyamidoamine dendrimers. *Electrophoresis* **2003**, *24*, 2733−2739.

(60) Zhang, C.; Tomalia, D. A. Gel electrophoretic characterization of dendritic polymers. In *Dendrimers and Other Dendritic Polymers*; Frechet, J. M. J., Tomalia, D. A., Eds.; John Wiley & Sons Ltd: New York, 2001; pp 239−253.

Table 1. Physicochemical Parameters of Generation 1 PAMAMs[a]

	G1.NH$_2$	G1.NHAc	G1.N(Gly)OH
theoretical MW	1430	1766	2614
MW measd by MALDI-TOF[b]	1430	1766	2468
M_n[c]	1398	1840	2385
M_w[c]	1431	1857	2411
polydispersity[c]	1.024	1.019	1.011
theoretical charge/mass ratio[d]			
pH = 8.3	5.59×10^{-3}		
pH = 2.5	9.79×10^{-3}	3.40×10^{-3}	5.36×10^{-3}
relative migration times (RSD)	0.94 (0.752%)	1.57 (1.01%)	1.19 (1.46%)
electrophoretic mobility (cm^2 V^{-1} s^{-1})	3.48×10^{-4}	2.08×10^{-4}	2.75×10^{-4}

[a] Data reprinted with permission from ref 61. Copyright 2005 Elsevier Science. [b] Obtained from the dominant peaks in MALDI-TOF spectra. [c] Measured by GPC. [d] Charge/mass ratios were calculated using the theoretical number of terminal and tertiary amine groups and theoretical molecular masses.

step as EDA is a bifunctional reactant; and (4) the residual EDA acts as a new core to initiate a trailing ($g - 1$) generation. Understanding the structural deviations of low generations is crucial for further characterization of higher generation PAMAMs.

We have synthesized generation 1 PAMAMs with acetamide (G1.NHAc) and hydroxyl (G1.N(Gly)OH) termini from the same starting material, an amine-terminated PAMAM (G1.NH$_2$), and analyzed the structural deviations of these PAMAM derivatives by CE as well as other techniques for comparison.[61] An ideal G1.NH$_2$ would contain 6 tertiary (−N≡) and 8 primary amines (−NH$_2$). Upon exhaustive acetylation, all the terminal amine groups are assumed to be transformed to acetamide groups, but the six tertiary amines remain intact. Similarly, when G1.NH$_2$ is reacted with excess glycidol, all terminal primary amines are expected to be transformed into tertiary amines (through secondary amines); thus the total theoretical number of tertiary amines in this molecule is 14, which is the sum of the original number of −N≡ and −NH$_2$ groups. Comparison of the analytical results of these derivatives to those of the parent dendrimer is necessary to determine the real composition.

Quantitative results regarding the purity and homogeneity can be achieved using CE based on the electrophoretic mobility of the components including charge distributions between the molecules. We analyzed these dendrimers using a bare fused silica capillary (i.d. = 75 μm, total length 64.5 cm, and effective length 56 cm) and internal standard 2,3-DAP. Figure 7 shows normalized CE electropherograms of G1.NH$_2$, G1.NHAc, and G1.N(Gly)OH. In the case of generation 1 PAMAMs with small molecular weight, huge adsorption of PAMAMs onto bare silica capillary surface is not expected. Therefore, bare silica capillary was used for the separation of G1 PAMAMs. Relative migration times (t_d/t_i, migration time ratio of dendrimers and 2,3-DAP) of all of these dendrimers are constant, and their relative standard deviation (RSD) values are all less than 2%,

indicating that good reproducibility has been achieved. Electrophoretic mobility of G1 PAMAM decreased after surface modifications, as expected. At pH 2.5, the observed electrophoretic mobility was in the order G1.NH$_2$ > G1.NGlyOH > G1.NHAc, i.e., in the same order as their theoretical net charge/mass ratio (Table 1). The peak shapes are also compared in Figure 7, where the main peaks of G1.NH$_2$ and G1.NHAc are much narrower than the G1.N-(Gly)OH peak. It can be clearly seen that the intensity of the main peak of G1.NHAc is much higher than that of G1.NH$_2$. After acetylation, there are more small visible peaks appearing in the G1.NHAc electropherogram (Figure 2), and the differences between various components of G1.NHAc seem to be magnified compared to the starting material G1.NH$_2$.

Deconvolution of the CE peaks using the PeakFit program (SYSTAT Software Inc., Point Richmond, CA 94804) provides more quantitative results. Figure 8 shows the deconvolution of G1.NH$_2$ (a), G1.NHAc (b), and G1.N(Gly)-OH (c) CE peaks in the presence of 2,3-DAP, and G1.NH$_2$ (d) in the absence of 2,3-DAP. Because the 2,3-DAP peak overlaps with G1.NH$_2$ peaks, deconvolution on the G1.NH$_2$ electropherogram was performed both in the presence and in the absence of 2,3-DAP (Figure 8a and Figure 8d). Deconvolution led to very similar profiles (see Figure 8a). The major peak, corresponding to the ideal G1.NH$_2$, represents 79.3% of the total peak area in Figure 8d, while in G1.NHAc (Figure 8b) the ideal component is 72.6% of the total peak area. G1.N(Gly)OH (Figure 8c) displays only one broad peak, as all the individual peaks are hidden under an envelope. Further MALDI-TOF spectrometry verifies that incomplete hydroxylation occurs even if 10 times excess of glycidol is added in the reaction mixture.[61] CE results indicate that, after acetylation, the differences between substituted PAMAM molecules are amplified, whereas the differences diminish after hydroxylation.

In order to compare the structural differences between PAMAM derivatives of higher generation to lower generations, we utilized amine-terminated PAMAM dendrimers of G4 as starting materials to synthesize acetyl, hydroxyl-terminated PAMAM derivatives.[62] We expect that high-

(61) Shi, X.; Bányai, I.; Islam, M. T.; Lesniak, W.; Davis, D. Z.; Baker, J. R., Jr.; Balogh, L. Generational, Skeletal and Substitutional Diversities in Generation One Poly(amidoamine) Dendrimers. *Polymer* **2005**, *46*, 3022−3034.
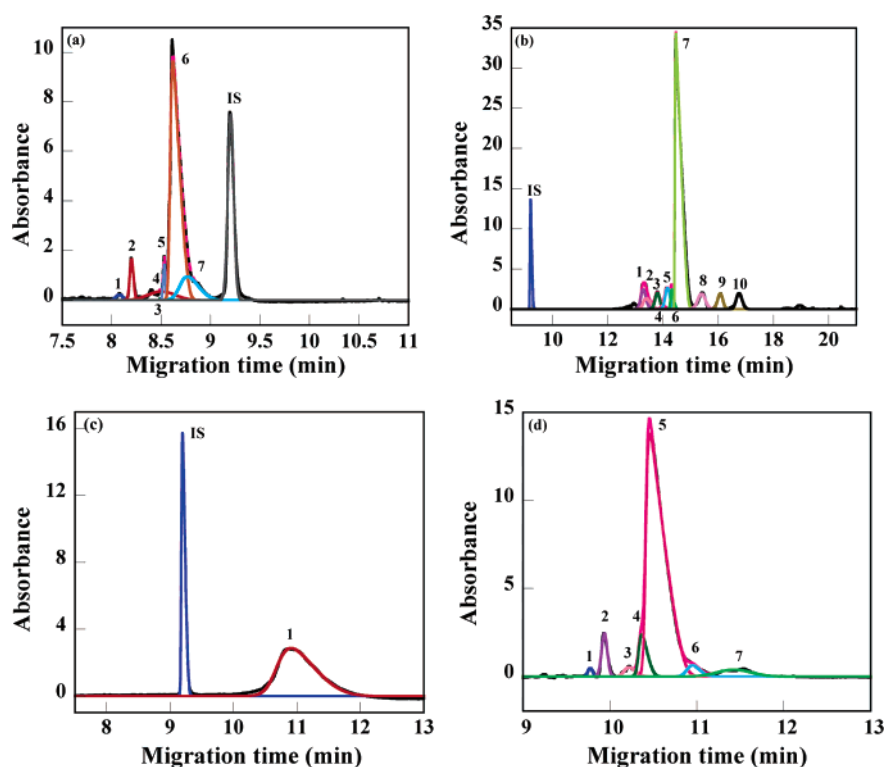
Figure 8. CE migration peaks of G1.NH$_2$ (a), G1.NHAc (b), and G1.N(Gly)OH (c) deconvoluted by PeakFit. Deconvoluted electropherogram of G1.NH$_2$ without internal standard is also shown in panel d. The major peak, corresponding to the pure G1.NH$_2$, possesses 79.3% of the total peak area in Figure 3d, while G1.NHAc constitutes 72.6% of the total peak area in Figure 3b. Regarding G1.N(Gly)OH (Figure 3c), there is only one major broad peak, representing all the components. Reprinted with permission from ref 61. Copyright 2005 Elsevier Science.

generation PAMAMs and derivatives will exhibit different properties compared to G1 dendrimers. Characteristically, density of the PAMAM molecules increases with generation and higher generation (G4 and above) PAMAM molecules have a close-to-spherical shape because of the exponentially growing number of terminal groups. With the growing number of terminal groups the relative differences become smaller, and the substitutional dispersity of higher generation PAMAMs may be masked in certain cases.

Both quantitative analysis and charge distribution evaluation of the PAMAM derivatives were performed by CE. Shown in Figure 9 are the CE electropherograms of G4.NH$_2$, G4.NHAc, and G4.N(Gly)OH. The migration peaks of polycationic G4 PAMAM derivatives were normalized using the average migration time of 2,3-DAP (11.8 min).[25] By comparing peak positions in the normalized electropherograms (Figure 9), the electrophoretic mobility of G4 PAMAM derivatives can be calculated. The electrophoretic mobility of G4 PAMAMs follows the order G4.NH$_2$ > G4.N(Gly)OH > G4.NHAc. Compared to CE studies of G1 PAMAMs, the substitutional dispersity of G4 PAMAM upon acetylation is not magnified as expected.[61] The structural
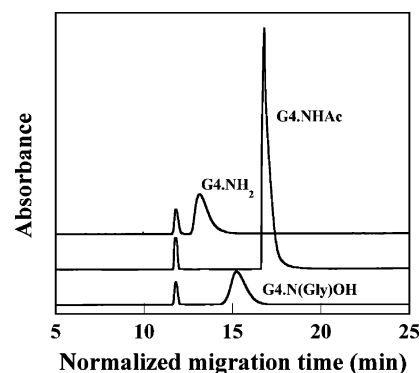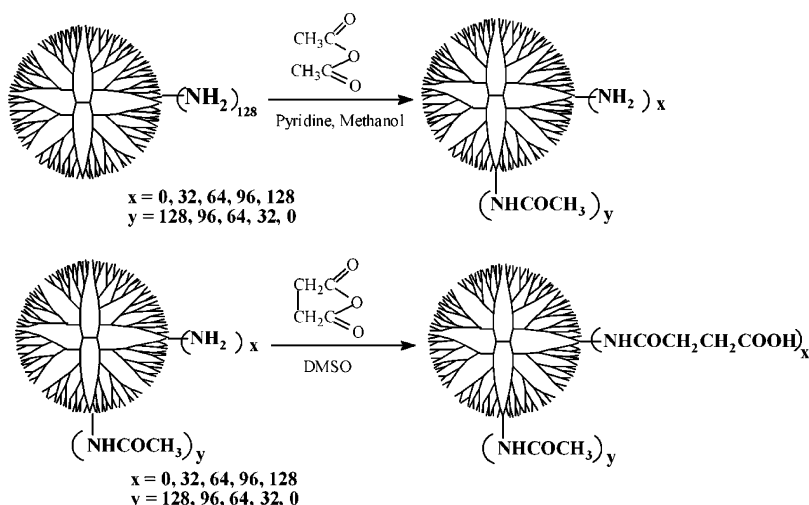
(62) Shi, X.; Lesniak, W.; Islam, M. T.; Muñiz, M. C.; Balogh, L.; Baker, J. R., Jr. Comprehensive Characterization of Surface-Functionalized Poly(amidoamine) Dendrimers with Acetamide, Hydroxyl, and Carboxyl Groups. *Colloids Surf., A*, submitted.

Figure 9. CE electropherograms of polycationic G4 and derivatives (G4.NH$_2$, G4.NHAc, G4.N(Gly)OH). The first peak corresponds to the internal standard 2,3-DAP. The electropherograms are normalized using the average migration time of 2,3-DAP (11.8 min).

dispersity of hydroxyl-terminated G4.N(Gly)OH remains masked the same as G1 PAMAMs.[61] The hidden substitutional dispersity of higher generation PAMAMs as well as their smaller generation counterparts mainly results from the incomplete hydroxylation reaction in nature. The incomplete hydroxylation produces mixtures of hydroxyl-terminated PAMAMs with very close molecular structures. Even at the G1 level, CE cannot differentiate the mixture of hydroxyl-terminated PAMAM derivatives with close molecular structures.[61]

Scheme 2. Schematic Representation of Acetylation and Carboxylation of G5.NH$_2$ PAMAM Dendrimer

x = 0, 32, 64, 96, 128
y = 128, 96, 64, 32, 0

x = 0, 32, 64, 96, 128
y = 128, 96, 64, 32, 0

6. Capillary Electrophoresis of Generation 5 (G5) with Defined Substitutions

The physicochemical properties of PAMAM dendrimers are intrinsically dependent on the generation number and surface functionalities. Compared with standard organic or inorganic colloidal particles, the surface charge of PAMAM dendrimers is inherently relevant to the polymer molecules themselves instead of that usually arising from ionic surfactants adsorbed onto particles during their preparation process. The surface charge of colloids plays a major role in their mobility and in migration behavior as their properties are often dominated by electrostatic interactions in aqueous solution. PAMAM dendrimers with systematically varied surface charges are expected to serve as a nearly ideal model for the investigation of electrophoretic mobility (EM).

Separation of organic and inorganic colloidal particles and biological vesicles may be of both analytical and preparative interest in environmental sciences, biomedicine, biotechnology, and industry. A broad range of colloids including polystyrene lattices,[63−65] silica sols,[66] semiconductor clusters,[67] bacterial particles,[68,69] and liposomes[70,71] have been separated by CE. We studied the EM of the same generation PAMAM dendrimers with different functionalities (which

is the case during the synthesis of multifunctional dendrimer nanodevices). This provides new insights on further characterization of PAMAM-based multifunctional nanodevices.

It is well established that the EM of linear polyelectrolytes is linearly proportional to their charge density at different zones.[72] For polyelectrolyte dendrimers, under otherwise identical instrument and run conditions, EM changes due to changes in pH and functionality or both. Charged PAMAM dendrimers, because of their nearly spherical shape, persistent size, and high concentration of nitrogen ligands in the interior and on the surface, are thought to exhibit behavior different from linear polyelectrolytes. On the other hand, dendrimer end group modifications with multifunctional moieties (drugs, targeting agents, imaging dyes) have been recently demonstrated to be extremely useful in targeted cancer therapy.[9,21,23,73,74] As highly charged macromolecules are often cytotoxic, the dendrimer effective charges have to be reduced and dendrimer-based multifunctional nanodevices

(63) VanOrman, B. B.; McIntire, G. L. Size-based separation of polystyrene nanoparticles by capillary electrophoresis. *Am. Lab.* **1990**, *22*, 66−67.

(64) Jones, H. K.; Ballou, N. Separations of chemically different particles by capillary electrophoresis. *Anal. Chem.* **1990**, *62*, 2484−2490.

(65) Petersen, S. L.; Ballou, N. E. Effects of capillary temperature control and electrophoretic heterogeneity on parameters characterizing separations of particles by capillary zone electrophoresis. *Anal. Chem.* **1992**, *64*, 1676−1681.

(66) McCormick, R. M. Characterization of silica sols using capillary zone electrophoresis. *J. Liq. Chromatogr.* **1991**, *14*, 939−952.

(67) Wang, Y.; Harmer, M.; Herron, N. Towards monodisperse semiconductor clusters-prepration and characterization of similar-to 13-angstrom thiophenolate-capped CdS clusters. *Isr. J. Chem.* **1993**, *33*, 31−39.

(68) Pfetsch, A.; Welsch, T. Determination of the electrophoretic mobility of bacteria and their separation by capillary zone electrophoresis. *Fresenius' J. Anal. Chem.* **1997**, *359*, 198−201.

(69) Baygents, J. C.; Glynn, J. R., Jr.; Albinger, O.; Biesemeyer, B. K.; Ogden, K. L.; Arnold, R. G. Variation of Surface Charge Density in Monoclonal Bacterial Populations: Implications for Transport through Porous Media. *Environ. Sci. Technol.* **1998**, *32*, 1596−1603.

(70) Radko, S. P.; Stastna, M.; Chrambach, A. Size-Dependent Electrophoretic Migration and Separation of Liposomes by Capillary Zone Electrophoresis in Electrolyte Solutions of Various Ionic Strengths. *Anal. Chem.* **2000**, *72*, 5955−5960.

(71) Duffy, C. F.; Gafoor, S.; Richards, D. P.; Admadzadeh, H.; O'Kennedy, R.; Arriaga, E. A. Determination of Properties of Individual Liposomes by Capillary Electrophoresis with Postcolumn Laser-Induced Fluorescence Detection. *Anal. Chem.* **2001**, *73*, 1855−1861.

(72) Gao, J. Y.; Dubin, P. L.; Sato, T.; Morishima, Y. Separation of polyelectrolytes of variable compositions by free-zone capillary electrophoresis. *J. Chromatogr., A* **1997**, *766*, 233−236.

(73) Majoros, I. J.; Thomas, T. P.; Mehta, C. B.; Baker, J. R., Jr. PAMAM Dendrimer-Based Multi-Functional Engineered Nanodevice for Cancer Therapy. *J. Med. Chem.*, in press.
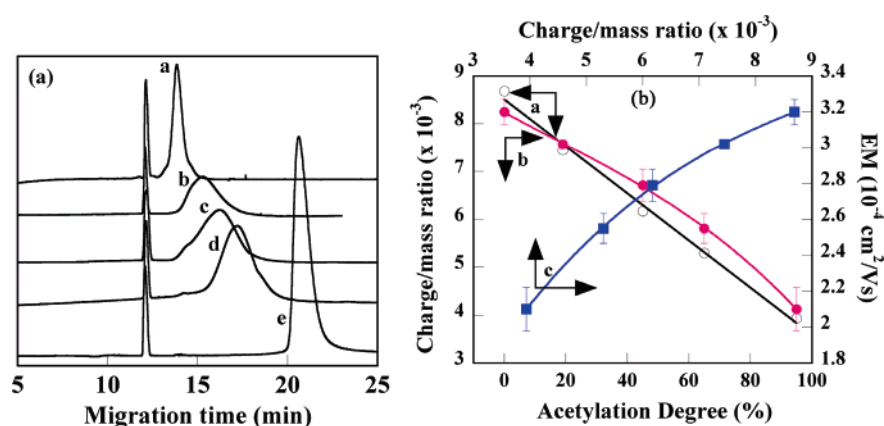
Figure 10. (a) Normalized electropherograms of acetylated G5 PAMAMs with acetylation percentage of 0% (a), 25% (b), 50% (c), 75% (d), and 100% (e). The first peak corresponds to the internal standard 2,3-DAP. (b) Measured charge/mass ratios of acetylated G5 PAMAMs as a function of practical acetylation degree (a), dependence of EM of acetylated G5 PAMAMs on the acetylation degree (b), and the plot of EM of acetylated G5 PAMAMs as a function of practical charge/mass ratio (c). Arrows indicate the appropriate axis.

Table 2. Physicochemical Parameters of G5 PAMAMs of Different Acetylation Degree

	G5.NH$_2$	G5.25Ac	G5.50Ac	G5.75Ac	G5.100Ac
theoretical acetylation percentage (%)	0	25	50	75	100
theoretical number of terminal amino groups	128	96	64	32	0
practical acetylation degree[a] (%)	0	19	45	65	95
practical number of terminal amino groups[a]	110	89	61	39	6
tertiary amine groups[a]	116	116	116	116	116
total amine groups	226	205	177	155	122
theoretical MW	28 826	30 170	31 514	32 858	34 202
practical M_n (SEC)	26 010	27 510	28 680	29 240	30 990
practical M_w (SEC)	28 730	29 880	31 150	32 150	32 840
polydispersity (SEC)	1.104	1.086	1.086	1.100	1.060
practical M_w (MALDI-TOF)	26 462	26 778	27 667	28 889	30 065
N/M_n[b]	8.689×10^{-3}	7.452×10^{-3}	6.172×10^{-3}	5.301×10^{-3}	3.937×10^{-3}
relative migration time ratio (T_d/T_s) (RSD, $n = 3$)	1.18 (2.75%)	1.25 (1.31%)	1.35 (4.22%)	1.48 (3.86%)	1.80 (8.07%)
normalized migration time[c] (min)	14.32	15.18	16.39	17.97	21.85
apparent EM ($10^{-4} \times$ cm^2 V^{-1} s^{-1})	3.2 ± 0.07	3.02 ± 0.02	2.79 ± 0.09	2.55 ± 0.08	2.10 ± 0.12
CE peak width at half-height[d] (min)	0.552	1.981	2.384	2.162	0.95

[a] Calculated by NMR and potentiometric acid—base titration. [b] Determined using molar mass measured using SEC. [c] Average migration time of 2,3-DAP is 12.14 min. [d] The CE peak width at half-height was obtained from Figure 10a under the same conditions.

must be prepared using partially modified PAMAM dendrimers as intermediate materials. Charge and charge distribution of partially modified dendrimers play an important role in determining physicochemical properties of the final products and influences their interactions with biologic entities.

PAMAM dendrimer derivatives with defined substitutions were synthesized from generation 5 amine-terminated (G5.NH$_2$) materials with a systematic change of their acetylation and carboxylation degrees using standard methods (Scheme 2). CE was employed to investigate the effect of charge on the EM of the polycationic and polyanionic

dendrimer molecules as well as the molecular distribution changes upon defined substitutions.[75]

CE Analysis of Acetylated G5 PAMAMs. Figure 10a shows the normalized electropherograms of the polycationic acetylated PAMAMs. Clearly, the migration time increases with the increase of acetylation degree, which is attributed to the decreased charge/mass ratio (summarized in Table 2). It is found that the migration peaks of partially acetylated G5 PAMAMs are much broader than those of nonacetylated (G5.NH$_2$) or of the fully acetylated G5.100Ac (see the CE peak width at half-height in Table 2). We have also found that although the practical charge/mass ratio of these poly-

(74) Majoros, I. J.; Myc, A.; Thomas, T. P.; Mehta, C. B.; Baker, J. R., Jr. PAMAM Dendrimer-Based Multi-Functional Engineered Nano-Device for Cancer Therapy. II: Synthesis, Characterization, and Functionality. *J. Med. Chem.*, in press.

(75) Shi, X.; Bányai, I.; Rodriguez, K.; Islam, M. T.; Lesniak, W.; Balogh, L.; Baker, J. R., Jr. Molecular Distribution and Electrophoretic Mobility Studies of Poly(amidoamine) Dendrimers of Defined Charges. *Anal. Chem.*, submitted.
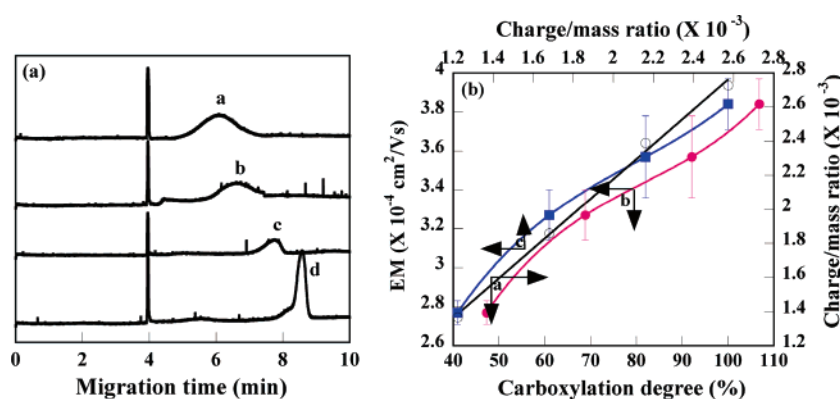
Figure 11. (a) Normalized electropherograms of carboxylated G5 PAMAMs having carboxylic acid termini of 25% (a), 50% (b), 75% (c), and 100% (d) of the available end groups. The first peak corresponds to MBA, the neutral marker. (b) Measured charge/mass ratios of carboxylated G5 PAMAMs as a function of practical carboxylation degree (a), dependence of electrophoretic mobility of carboxylated G5 PAMAMs on the carboxylation degree (b), and the plot of electrophoretic mobility of carboxylated G5 PAMAMs as a function of practical charge/mass ratio (c). Arrows indicate the appropriate axis.

Table 3. Physicochemical Parameters of G5 PAMAMs of Different Carboxylation Degree

	G5.25SA	G5.50SA	G5.75SA	G5.100SA
theoretical carboxylation degree (%)	25	50	75	100
theoretical surface carboxyl groups	32	64	96	128
practical carboxylation degree[a] (%)	41	61	82	100
practical surface carboxyl groups[a]	45	67	90	110
theoretical MW	36 058	37 914	39 770	41 626
practical M_n (SEC)	32 910	36 050	37 650	40 330
practical M_w (SEC)	34 390	38 660	41 250	42 500
polydispersity (SEC)	1.045	1.072	1.096	1.054
practical MW (MALDI-TOF)	31 222	32 333	33 889	35 111
N/M_n[b]	1.367×10^{-3}	1.859×10^{-3}	2.390×10^{-3}	2.727×10^{-3}
relative migration time ratio (T_d/T_s) (RSD, $n = 3$)	1.57 (1.94%)	1.74 (3.68%)	1.91 (4.14%)	2.04 (5.15%)
EM ($10^{-4} \times cm^2 V^{-1} s^{-1}$)	2.77 ± 0.06	3.27 ± 0.13	3.27 ± 0.21	3.84 ± 0.13
CE peak width at half-height[c] (min)	1.300	1.139	0.502	0.277

[a] Calculated by NMR and acid−base titration. [b] Determined using molar mass measured using SEC. [c] The CE peak width at half-height was obtained from Figure 11a under the same conditions.
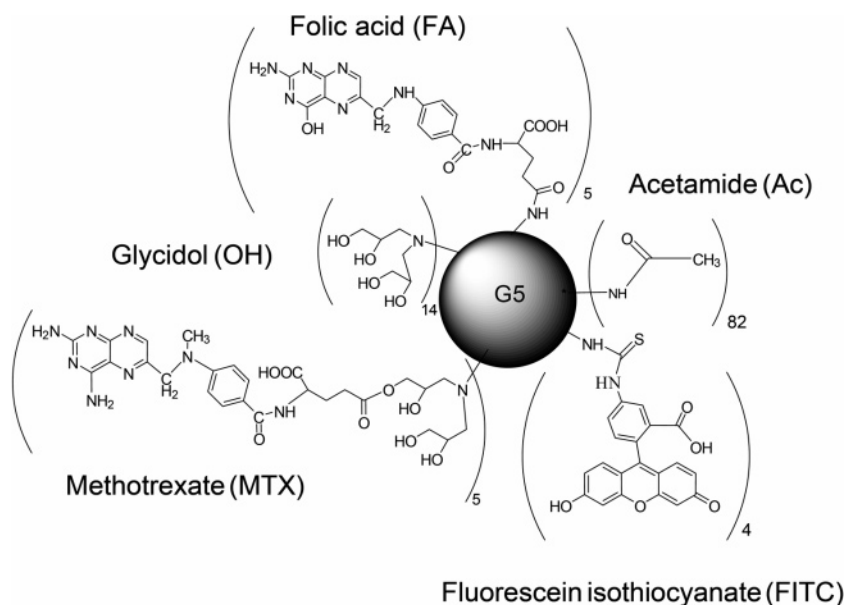
cationic dendrimers (determined by ^{1}H NMR and titration) decreases linearly (Figure 10b, curve a) with the increase of acetylation degree, their EMs decrease nonlinearly, in a concave downward shape (Figure 10b, curve b), which indicates that the difference in their charge/mass ratios is not solely responsible for the migration rate differences of the PAMAM dendrimer derivatives. If we plot the change of their EMs as a function of charge/mass ratio, the same nonlinear change is also observed (see Figure 10b, curve c).

CE Analysis of Carboxylated G5 PAMAM Dendrimers. Bare silica capillary was used to separate carboxylated G5 PAMAMs with mixed acetyl and carboxyl groups. The average migration time of methoxybenzyl alcohol (MBA) (3.96 min, 25 runs) was used to normalize the peak positions of the carboxylated G5 PAMAMs. Figure 11a shows the normalized electropherograms of these polyanionic PAMAMs. It is clear that the migration time of these PAMAMs increases with the increase of carboxylation degree, which is ascribed to the increased charge/mass ratio, resulting in their increased EMs (shown in Table 3). We found that the migration peak of partially carboxylated G5

PAMAMs is much broader than the migration peak of 100% carboxylated G5 dendrimer (see the CE peak width at half-height in Table 3). This is consistent with the broader substitutional distribution of acetylated PAMAMs as described above (carboxylate groups do not interact with the negatively charged capillary wall). We also found that the practical charge/mass ratio versus carboxylation degree is linear (Figure 11b, curve a), while their EMs as a function of both carboxylation degree (Figure 11b, curve b) and charge/mass ratio (Figure 11b, curve c) are nonlinear, in an "S" shape, indicating that, besides the role played by the charge/mass ratio, additional mechanisms are also involved in their separation.

The molecular *charge distribution* changes significantly after dendrimer surface modifications as confirmed by CE analysis. Partially modified G5 PAMAMs have much broader overall distribution than those of fully modified or nonmodified G5 dendrimers due to the increase in the substitutional distribution. This can be reasoned as follows: Full-generation amine-terminated dendrimer materials are the mixture of at least three major components, namely, the ideal structure

Scheme 3. Structure of a Trifunctional Dendrimer Conjugate (G5-Ac-FITC-FA-OH-MTX[e])[a]

[a] The central circle represents EDA-core generation 5 PAMAM dendrimer. Subscripts outside braces indicate average numbers of small molecules covalently attached to the dendrimer surface.

(dominant component, >90%) and different close-to-ideal structures (trailing generation and dimers, usually totaling <10%). Partially derivatized dendrimers (even in an idealized case) have a secondary distribution of substituents over these primary components, because of the stochastic nature of this substitution reaction. Consequently, the highest charge distribution ensues when 50% of the surface functionalities are substituted. Similar results showing broad distribution for partially modified G2.NH2 PAMAM dendrimers with 1,2-epoxyhexane have also been demonstrated by using ESI-MS spectra analysis.[76]

EM is usually linearly dependent on the charge/mass ratio of the studied materials. It often changes when different mechanisms are involved in the separation process. Regarding the nonlinear increase of EM (concave downward shape shown in Figure 10b) of G5 PAMAM acetamides, there may be several factors influencing their separation. (1) Adsorption−desorption of dendrimers onto the capillary surface: Silanization coating onto the capillary internal surface cannot exclude the complete desorption of polycationic PAMAM dendrimers onto the quartz surface.[25,56] We think that the differential adsorption/desorption process of PAMAM polycations onto the internal surface of the capillary could be responsible for the nonlinear change in EMs. Namely, G5 PAMAM acetamides with lower acetylation degree (higher charge/mass ratio) display much stronger adsorption on the capillary surface than that of G5 PAMAM acetamides with higher acetylation degree. Consequently, the EMs of G5 PAMAM acetamides with higher charge/mass ratio are slightly reduced. (2) Counterion binding onto charged

dendrimer spheres: As demonstrated by Manning's theory[49] and confirmed later by Dubin and co-workers' studies[45,46,72] on linear and dendrimeric polyelectrolytes using capillary electrophoresis, counterion condensation around polyelectrolytes strongly influences their electrokinetic mobility. In our case, acetylated G5 PAMAMs bearing more terminal amine groups may experience higher counterion binding force during electrophoresis, which also contributes to the concave downward nonlinear increase of EMs as a function of charge/mass ratio. (3) Dendrimer hydrodynamic size: On the basis of previous work,[27] an increasing number of acetyl termini leads to the shrinkage of the dendrimer molecule. We expect that larger dendrimer spheres experience a larger inhibition force during the electrophoresis, and the acetylated G5 PAMAMs having more acetamide groups experience less hindrance than those bearing more terminal amine groups. The combination of the above three factors may contribute to the nonlinear EM increase of acetylated G5 PAMAMs with the increase of charge/mass ratio.

For G5 PAMAM succinamic acids, the same nonlinear (S shape upward) increase of their EMs as a function of charge/mass ratio was observed. The same factors as discussed above (factors 2 and 3) for G5 PAMAM acetamides may result in the nonlinear change of their EMs. Regarding factor 3, it is also expected that G5 PAMAM succinamic acids with higher carboxylation degree have larger hydrodynamic sizes,[27] and they may receive higher hindrance during the electrophoretic migration. However, compared to acetylated G5 PAMAM polycations, carboxylated G5 PAMAM polyanions have no electrostatic interaction with the capillary surface at running buffer of pH 8.3,[26] which means that factor 1 discussed above for G5 PAMAM acetamides does not apply in this case. Hence, for G5

(76) Zhang, C.; O'Brien, S.; Balogh, L. Comparison and Stability of CdSe Nanocrystals Covered with Amphiphilic Poly(Amidoamine) Dendrimers. *J. Phys. Chem. B* **2002**, *106*, 10316−10321.
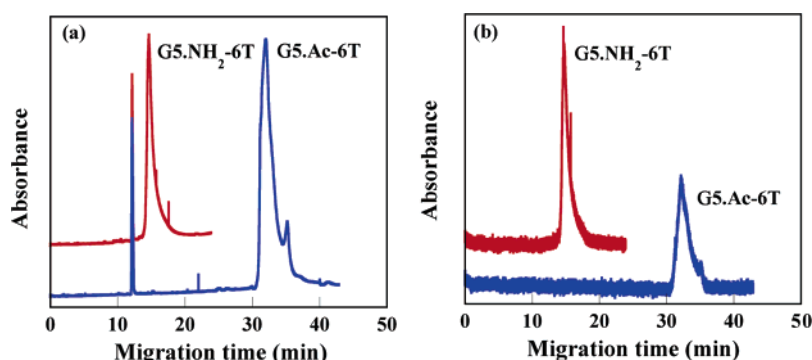
Figure 12. Normalized electropherograms of G5.NH2-6T and G5.Ac-6T at 210 nm (a) and 520 nm (b).
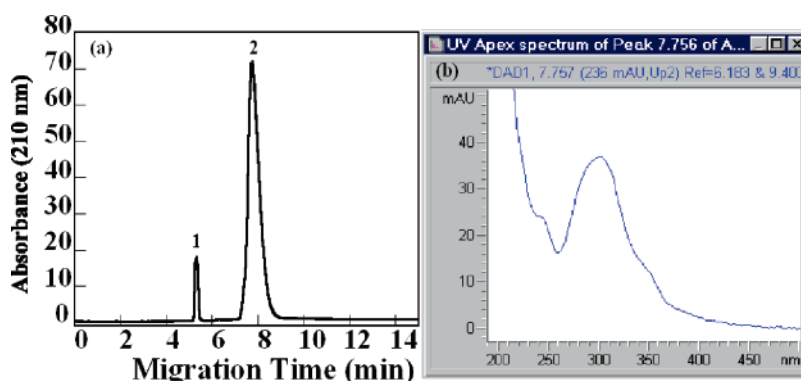

Figure 13. A typical electropherogram (a) of G5.NGlyOH-FA$_5$-MTX$_{10}$ conjugates detected at 210 nm using a silanized silica capillary (i.d. 100 μm) with effective length of 40 cm and total length of 48.5 cm. Peaks 1 and 2 correspond to the internal standard 2,3-DAP and G5.NGlyOH-FA$_5$-MTX$_{10}$ conjugates, respectively. A UV−vis spectrum analysis of peak 2 is also shown (b).

PAMAM succinamic acids, counterion binding onto charged dendrimer spheres and dendrimer hydrodynamic sizes may play a major role in influencing their nonlinear increase of EMs with increasing charge/mass ratio.

In summary, a systematic set of acetylated and carboxylated G5 PAMAM dendrimers with defined charges were used as a model system to investigate electrokinetic mobilities of dendrimer molecules as a function of charge and structure. Partially modified dendrimers exhibit a broader migration peak in their capillary electropherograms than fully modified or nonmodified dendrimers do due to the increased substitutional distribution. The nonlinear EM changes of both the polycationic G5 PAMAM acetamides and polyanionic G5 PAMAM succinamic acids with charge/mass ratio indicates complex separation mechanisms. Factors influencing the separation of these dendrimers could also be delineated through theoretical calculations, which is currently in progress in our group.

7. Capillary Electrophoresis of Mono- and Multifunctional Complex Dendrimer Medical Nanodevices

PAMAM dendrimers are ideal nanoplatforms to conjugate a defined number of targeting moieties, dye tags, and drugs for multifunctional targeting, imaging, and treatment of biological systems. A novel PAMAM dendrimer-based
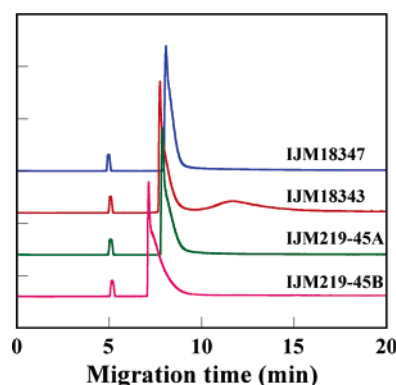

Figure 14. Capillary electropherograms of several dendrimer-based nanodevices. IJM18347: G5-Ac$_{82}$-FITC$_5$-FA$_5$-MTX$^e_5$-(GlyOH)$_n$. IJM18343: G5-Ac$_{82}$-FA$_5$-MTX$^e_5$-(GlyOH)$_n$ (unpurified). IJM219-45A: G5-Ac$_{89}$-FA$_{3.5}$-MTX$^e_{4.8}$-(GlyOH)$_n$. IJM219-45B: G5-Ac$_{70}$-FA$_y$-MTX^e_z-(GlyOH)$_m$.

cancer therapy agent carrying biospecific targeting moieties (e.g., folic acid), fluorescent dyes, and drugs have been developed at the Center for Biologic Nanotechnology, University of Michigan.[21−23,73,74,77,78] For instance, Scheme 3 shows the molecular structure of a multifunctional G5

(77) Patri, A. K.; Thomas, T.; Baker, J. R., Jr.; Bander, N. H. Antibody-dendrimer conjugates for targeted prostate cancer therapy. *Polym. Mater.: Sci. Eng.* **2002**, *86*, 130.
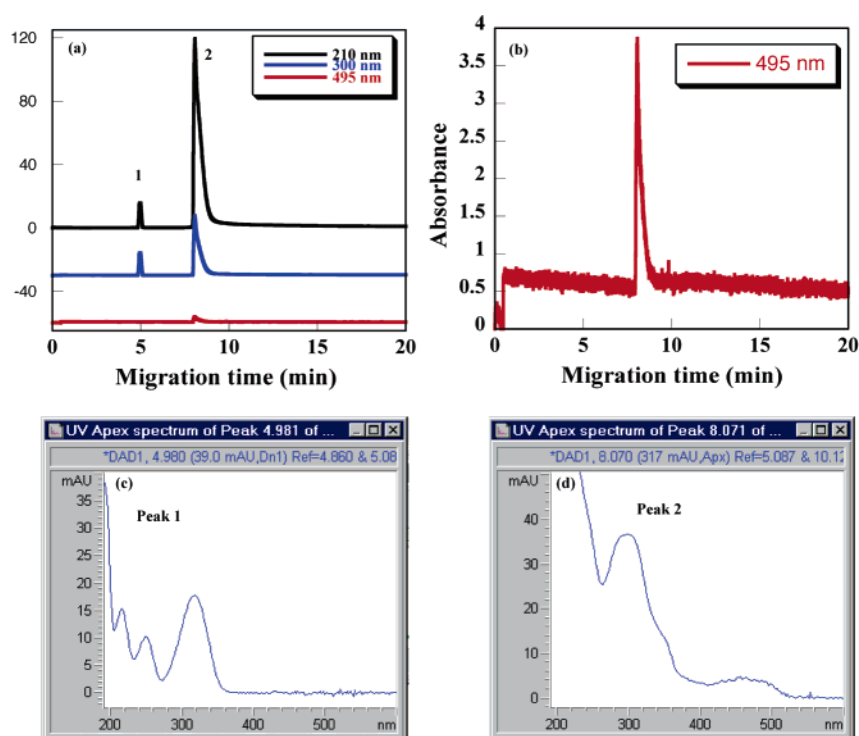
Figure 15. (a) CE electropherograms of a trifunctional PAMAM nanodevice (G5-Ac$_{82}$-FITC$_5$-FA$_5$-MTX$^e_5$-(GlyOH)$_n$) detected at 210, 300, and 495 nm, (b) a magnified electropherogram at 495 nm, (c) off-line UV spectrum of peak 1 (internal standard), and (d) off-line UV spectrum of peak 2 (nanodevice) shown in panel a.

dendrimer nanodevice conjugated with folic acid (FA), methotrexate (MTX), and fluorescein isothiocyanate (FITC) molecules.[31] It is established that these dendrimer nanodevices can effectively transverse vascular pores and directly infuse tumor cells.[21] Other group have also developed folic acid−dendrimer conjugates to target tumor cells expressing high-affinity folate receptors, and demonstrated that folate-conjugated magnetic resonance imaging contrast agents represent a promising new approach for tumor targeting.[79,80] Although the research on medical applications of dendrimer-based nanodevices continues progressively, the characterization of these multifunctional dendrimer nanodevices still remains a great challenge. Substitutional dispersity of multifunctional dendrimer-based nanodevices is often expected due to the multistep surface modifications with different functional moieties.

As opposed to other techniques, CE displays several advantages: (1) both purity and charge distribution can be simultaneously evaluated; (2) the on-capillary UV−vis diode array detector allows detection using multiple wavelengths; and (3) a spectrum analysis of each individual migration peak is available.

We first demonstrated that monofunctional dendrimer−dye conjugates could be analyzed by the developed CE method.[25] G5-6T (6-carboxytetramethyl-rhodamine) conjugates[81,82] with both amino and acetamide termini were synthesized for biosensing purposes[75] and analyzed using CE. The detection wavelengths were selected as 210, 250, 280, and 520 nm. The 520 nm wavelength is the maximum absorbance of 6T dye molecules. Figure 12 shows the normalized electropherograms of G5.NH$_2$-6T and G5.Ac-6T conjugates at both 210 nm (a) and 520 nm (b). It is clear that both G5.NH$_2$-6T and G5.Ac-6T materials exhibit similar peak shapes at two different wavelengths, indicating that the materials are quite homogeneous. The CE peak at 520 nm (see Figure 12b) further supports the presence and distribution of 6T moieties, because at 520 nm only 6T moieties have absorbance.

Bifunctional G5.NGlyOH-FA$_5$-MTX$_{10}$ nanodevices were analyzed using CE.[75] To determine different moieties at-

(78) Thomas, T. P.; Majoros, I. J.; Kotlyar, A.; Kukowska-Latallo, J. F.; Bielinska, A.; Myc, A.; Baker, J. R., Jr. Targeting and Inhibition of Cell Growth by an Engineered Dendritic Nanodevice. *J. Med. Chem.*, in press.

(79) Konda, S. D.; Aref, M.; Wang, S.; Brechbiel, M.; Wiener, E. C. Specific targeting of folate-dendrimer MRI contrast agents to the high affinity folate receptor expressed in ovarian tumor xenografts. *Magma* **2001**, *12*, 104−113.

(80) Wiener, E. C.; Konda, S.; Shadron, A.; Brechbiel, M.; Gansow, O. Targeting dendrimer-chelates to tumors and tumor cells expressing the high-affinity folate receptor. *Invest. Radiol.* **1997**, *32*, 748−754.

(81) Thomas, T. P.; Patri, A. K.; Myc, A.; Myaing, M. T.; Ye, J. Y.; Norris, T. B.; Baker, J. R.; Jr. In Vitro Targeting of Synthesized Antibody-Conjugated Dendrimer Nanoparticles. *Biomacromolecules* **2004**, *5*, 2269−2274.

(82) Patri, A. K.; Myc, A.; Beals, J.; Thomas, T. P.; Bander, N. H.; Baker, J. R., Jr. Synthesis and in Vitro Testing of J591 Antibody-Dendrimer Conjugates for Targeted Prostate Cancer Therapy. *Bioconjugate Chem.* **2004**, *15*, 1174−1181.

tached onto dendrimer surfaces, suitable wavelengths (210, 240, 300, 350 nm) of the on-capillary UV−vis diode array detector were selected. The selection was based on the UV−vis spectrum of G5.NGlyOH-FA$_5$-MTX$_{10}$ conjugates collected in the CE running buffer (pH 2.5 phosphate buffer, 50 mM); 210 nm was used to detect the dendrimer aliphatic backbone, while 240 and 300 nm were used for MTX and FA moiety analysis, respectively. Figure 13a shows a typical CE electropherogram of G5.NGlyOH-FA$_5$-MTX$_{10}$. One can clearly see that the conjugate exhibits a monomodal symmetrical migration peak. The material is pure, because no impurity peaks are present in the electropherogram, even at a long separation time up to 50 min. To determine the real composition of the conjugate, offline UV−vis spectrometry analysis using Agilent software was performed (Figure 13b). The UV−vis spectrum of peak 2 related conjugate species (Figure 13b) is consistent with the UV−vis spectrum of G5.NGlyOH-FA$_5$-MTX$_{10}$ conjugates as measured by UV−vis spectrometry,[75] further indicating that peak 2 corresponds to the studied G5.NGlyOH-FA$_5$-MTX$_{10}$ conjugates.

Bifunctional and trifunctional dendrimer nanodevices containing FA, MTX, and FITC (Scheme 3) have also been analyzed by CE. Figure 14 shows electrophoregrams of several multifunctional G5-based nanodevices detected at 210 nm. Both purity (see electropherogram of IJM18343 in Figure 14) and molecular distribution can be evaluated using CE. The synthesis of dendrimer nanodevices is reproducible, as can be seen in the CE electropherograms of all the analyzed dendrimer nanodevices (Figure 14). The relative migration times of IJM18347, IJM18343, and IJM219-45A are close to each other, as they have similar charge/mass ratios. IJM219-45B has a shorter relative migration time due to its lower acetylation degree (only 70 amine groups have been acetylated). In order to further confirm the composition of the moiety distribution of dendrimer nanodevices, off-line UV spectral analysis can be performed using Agilent software. Figure 15 shows the CE electropherograms of a

trifunctional PAMAM nanodevice (G5-Ac$_{82}$-FITC$_5$-FA$_5$-MTX$^e_5$-(GlyOH)$_n$) detected at 210, 300, and 495 nm (Figure 15a) (all organic structures adsorb the 210 nm light, while 300 nm FA and MTX dominates, and at 495 nm only FITC can be observed). The material displays a single nonlinear peak at all wavelengths indicating that FITC, FA, and MTX moieties are equally present in all species. A magnified electropherogram (b) shows the distribution of the FITC moiety. Off-line UV spectra of peak 1 (c) and peak 2 (d) further confirm the peak compositions related to the internal standard and the analyzed nanodevice.

8. Concluding Remarks

This review has described the application of CE for the analysis of diverse PAMAM dendrimer nanoparticles ranging from amine-terminated PAMAMs, carboxyl-terminated PAMAMs, fully modified PAMAMs of different generation and functionalities, PAMAMs of defined substitutions, and multifunctional PAMAM-based medical nanodevices. As one of the analytical techniques, CE has been demonstrated to be a vital tool to analyze PAMAM dendrimer nanoparticles for medical applications. Purity, electrophoretic mobility, and molecular charge distribution of various PAMAM dendrimer nanoparticles can be assessed using CE. As dendrimers are continuously recognized as powerful nanoplatforms for biological nanotechnologies used for treatment, diagnosis, monitoring, and control of biological systems, we envision that CE will continuously play an important role to evaluate and analyze various novel multifunctional dendrimer nanodevices for detection, targeting, drug delivery, treatment, and therapeutics in various biological systems.

MP0500216